Med Mol Morphol (2012) 45:206–213
DOI 10.1007/s00795-011-0561-4

ORIGINAL PAPER

Chun-Ying Yang · Toshiyuki Matsuzaki · Norio Iijima
Naoko Kajimura · Hitoshi Ozawa

Morphofunctional changes of the astrocyte in rat hippocampus under different corticosteroid conditions

Received: March 25, 2011 / Accepted: August 12, 2011

Abstract In the present study, we examined the changes in the morphofunction of astrocytes in rat hippocampus under different circulating corticosteroid conditions by immunohistochemistry analysis of glial fibrillary acidic protein (GFAP) and ultra-high-voltage electron microscopy. Each GFAP-immunoreactive cell showed a hypertrophic appearance with well-developed thicker fibrous processes, and the number and the density of GFAP-immunoreactive cells were increased 4 weeks after adrenalectomy, whereas the changes were restored to the sham-control level with corticosterone replacement. The morphometric changes were observed in particular around the pyramidal neurons of CA1 and in the subgranular layer of dentate gyrus. The quantitative analysis clearly showed a significant increase in the number and the density of GFAP-immunoreactive cells in the adrenalectomy group; following corticosterone replacement, these increases were returned to the sham-control level. These changes were also specifically revealed by stereo-observation with ultra-high-voltage electron microscopy. The astrocyte showed more complicated fine three-dimensional branching after adrenalectomy. These results suggested that both the structure and function of astrocytes were modulated by corticosteroids via glucocorticoid receptor.

Key words Astrocyte · Glucocorticoid · Adrenalectomy · Immunohistochemistry · Ultra-high-voltage electron microscopy

C.-Y. Yang (✉) · T. Matsuzaki · N. Iijima · H. Ozawa
Department of Anatomy and Neurobiology, Nippon Medical School, 1-1-5 Sendagi, Bunkyo-ku, Tokyo 113-8602, Japan
Tel. +81-3-3822-2131; Fax +81-3-5685-6640
e-mail: yangchun@nms.ac.jp

C.-Y. Yang
The Faculty of Medicine, Beihua University, Jilin City, China

N. Kajimura · H. Ozawa
Research Center for Ultra-High Voltage Electron Microscopy, Osaka University, Osaka, Japan

Introduction

It is well known that the hippocampus contains the highest density of glucocorticoid receptors (GR, type II) and mineralocorticoid receptors (MR, type I), both in neurons[1–8] and in glial cells.[9–14] Therefore, the hippocampus is thought to be a significant target of corticosteroids. The effects of corticosteroids on hippocampal neurons, especially on pyramidal neurons and granular neurons of the dentate gyrus, which express glucocorticoid receptors (GR), have been well studied. Many previous studies reported that the hippocampal neurons show several morphological and functional changes under different corticosteroid conditions. For example, an adrenalectomy (ADX) is well known to induce degeneration or death of hippocampal neurons.[15–18] Several studies also have analyzed the effect of glucocorticoid on glial cells, especially on astrocytes.[19–21] Astroglia, once overlooked as merely supportive elements, have recently been reevaluated because glial cells have been reported to integrate neuronal inputs and modulate synaptic activities.[22–27] Therefore, it is equally important to determine the changes of astrocytes associated with the morphofunctional changes of neurons regulated by glucocorticoid. Nichols et al.[28] reported that the decrease in GFAP mRNA and protein, a marker for astrocytes, by corticosterone in vivo is directly mediated via GR. They also indicated that most of the glucocorticoid responses cloned by differential hybridization were more strongly expressed in glial cells than in neurons.[29] O'Callaghan et al.[19] observed increases in GFAP protein and GFAP mRNA in hippocampus and cortex after ADX found by radioimmunoassay and a blot hybridization analysis. An increase in the density of GFAP-immunoreactive (GFAP-ir) cells in the granule cell layer after ADX with immunohistochemistry was reported by Gould et al.[20] Krugers et al.[21] reported that the size and shape of astroglial cells were changed following ADX. However, they did not performed detailed quantitative analysis. Thus, there are no reports about the changes of astroglias under different corticosteroid conditions with detailed quantitative morphometric analysis. In the present study, we examined the detailed morphological changes of

glial cells around each specific hippocampal region under different corticosteroid conditions by immunohistochemical methods, and we also investigated by detailed quantitative morphometric analysis. Additionally, the fine structural changes of the astrocytes under different corticosteroid conditions were observed by ultra-high-voltage electron microscopy for three-dimensional detail.

Material and methods

Animals

Adult male Wistar rats (200–250 g in body weight; Saitama Experimental Animals Supply, Japan) were used in this study. They were housed in an air-conditioned room (23° ± 1°C) under 12-h light (0700–1900)/12-h dark (1900–0700) cycles with free access to food and water. Animals were divided into three experimental groups as follows: (1) sham-operated control group; (2) bilaterally adrenalectomized (ADX) 4-week group (received 0.9% saline as their drinking water); (3) subcutaneously implanted corticosterone single pellet (200 mg for 90 days, 2.22 mg/day; Innovative Research of America) for 2 weeks to ADX 2-week group (received 0.9% saline as their drinking water). All procedures in this study were in accordance with the Committee on Animal Bio-Ethics of Nippon Medical School.

Immunohistochemistry

Four rats for each experimental group were used for the immunohistochemical study. Animals were deeply anesthetized with an intraperitoneal injection of sodium pentobarbital (50 mg/kg body weight). They were perfused through the left ventricle with physiological saline, followed by a mixture of 4% paraformaldehyde and 0.2% picric acid in 0.1 M phosphate buffer (PB, pH 7.4). The brain was quickly removed from the skull and postfixed in the same fixative overnight. Then, the brain was immersed in 0.1 M PB (pH 7.4) containing 30% sucrose at 4°C for 3 days for cryoprotection. The brains were frozen by –60°C *n*-hexane, and serial frontal sections were cut at 25 μm with a cryostat (Leica CM 3050S Microsystems, Nussloch, Germany). The sections were treated in 0.01 M $NaIO_4$ solution for 20 min to block remaining endogenous peroxidase activity. After washing in 0.1 M phosphate-buffered saline (PBS) containing 0.3% Triton X-100 (TPBS, pH 7.4), the sections were preincubated in a 10% normal goat serum under microwave irradiation (200 W, 5-s intermittent irradiation; Azumaya, Tokyo, Japan) for 10 min. Then, the sections were incubated with rabbit anti-GFAP serum (1:1,000; Chemicon International, CA, USA) for 30 min under microwave irradiation. After being washed in TPBS, the sections were reacted with biotinated anti-rabbit IgG (Nichirei, Tokyo, Japan) for 10 min under microwave irradiation. After washing in TPBS, the sections were reacted with streptoavidin–biotin complex for 10 min under microwave irradiation. The sections were then washed in PBS, and reacted with 0.05% 3,3′-diaminobenzidine solution (DAB) in Tris-HCl buffer containing 0.01% H_2O_2. Finally, the sections were rinsed in 0.1 M PBS and mounted on gelatin-coated glass slides, dried, and covered with a coverslip.

Quantitative analysis of the number and density of GFAP-ir cells

The number of GFAP-immunoreactive (GFAP-ir) cells and the density of GFAP-ir cells around the hippocampus were estimated. For these measurements, five sections per animal in identical fields from serial sections were used. The number of GFAP-ir cells was analyzed in three regions per section: (1) stratum oriens and stratum radiatum of the peripyramidal cell layer of CA1; and (2) supragranular (molecular) and (3) subgranular (polymorphic cell) layers of the dentate gyrus. Briefly, the images of sections were captured with a microscopic digital camera (DP 70; Olympus) in an Olympus microscope (AX80 TRF), with a 300 μm × 300 μm frame. Special care was taken to place the frame in a similar location on each section for each animal under strictly identical conditions in terms of light illumination. The frame size was kept constant throughout the whole study. The number of GFAP-ir cells was counted with these captured images (9×10^4 μm^2). The values were expressed as mean ± SEM. Statistical analysis for the number of GFAP-ir astrocytes in the experimental groups for each region was performed by one-way analysis of variance (ANOVA). Moreover, the density of GFAP-ir was analyzed using ImageJ software. Gray-level values were obtained after the same degree of subtraction of background staining for each section. Each image was converted to gray-scale and the threshold for detecting the optical gray density was set to the same level, to ensure that all relevant staining was included in the analysis. The mean value from the histogram, which is a measure of brightness, was used as a quantitative measure of the density of GFAP-ir within the area inside the frame. The density of the three experimental groups was statistically analyzed using ANOVA.

Ultra-high-voltage electron microscopy

Three experimental group animals ($n = 4$) were used for Golgi impregnation for ultra-high-voltage electron microscopy after the procedures of Hama et al.[30] Briefly, animals were deeply anesthetized by intraperitoneal injection of sodium pentobarbital (50 mg/kg in body weight). Brains were perfused through the left ventricle of the heart with a physiological saline solution followed at 20-min intervals by the fixative of 4% paraformaldehyde and 1% glutaraldehyde in 0.1 M PB (pH 7.2), and then 2.5% paraformaldehyde, 2.5% glutaraldehyde in 0.1M PB. After fixation, the brain was removed from the skull and postfixed in the same fixative overnight.

Sections 200 μm thick were cut by a microslicer (D.S.K. DTK-3000). After several rinses in 0.1 M cacodylate buffer followed by brief rinses in 2.5% potassium dichromate, the sections were immersed for 3 days in a mixture of 2.3% potassium dichromate and 0.4% osmium tetroxide at 20°C. Then, the sections were immersed in a solution of 0.7% silver nitrate at 20°C for 3 days. Following dehydration in a

graded ethanol series and treatment with propylene oxide, the sections were flat-embedded on siliconized glass slides in Quetol 812 at 45°C for 1 day, and then at 60°C for 2 days. The embedded sections were examined under a stereoscopic microscope to select the Golgi-impregnated glia. Small pieces of sections containing recorded cells around the CA1 region of the pyramidal cell layer mounted on epoxy blocks were cut with a Leica ultracut UCT at 5-μm thickness and mounted on 75-mesh nickel grids. Specimens were then observed in a Hitachi H-3000 electron microscope operated at 3,000 kV. The observed glial cells were oriented roughly parallel to the Y-axis of the image field. Three pictures, a zero tilt and ± 8°tilt, were taken with the original magnification of 3,000×.

Results

Changes in expression of GFAP-immunoreaction (-ir), particularly in the peripyramidal area of CA1, stratum oriens, and stratum radiatum, and supragranular (molecular layer) and subgranular (polymorphic cell) layers of the dentate gyrus, were investigated. In the sham-control group, GFAP-ir was distributed throughout the entire hippocampus, although some differences in the density of immunoreactivity were observed from layer to layer (Fig. 1A). The most abundant GFAP-ir was observed in the polymorphic cell layer of the dentate gyrus. The least GFAP-ir was observed in the pyramidal and the granular neuronal layers. Although the

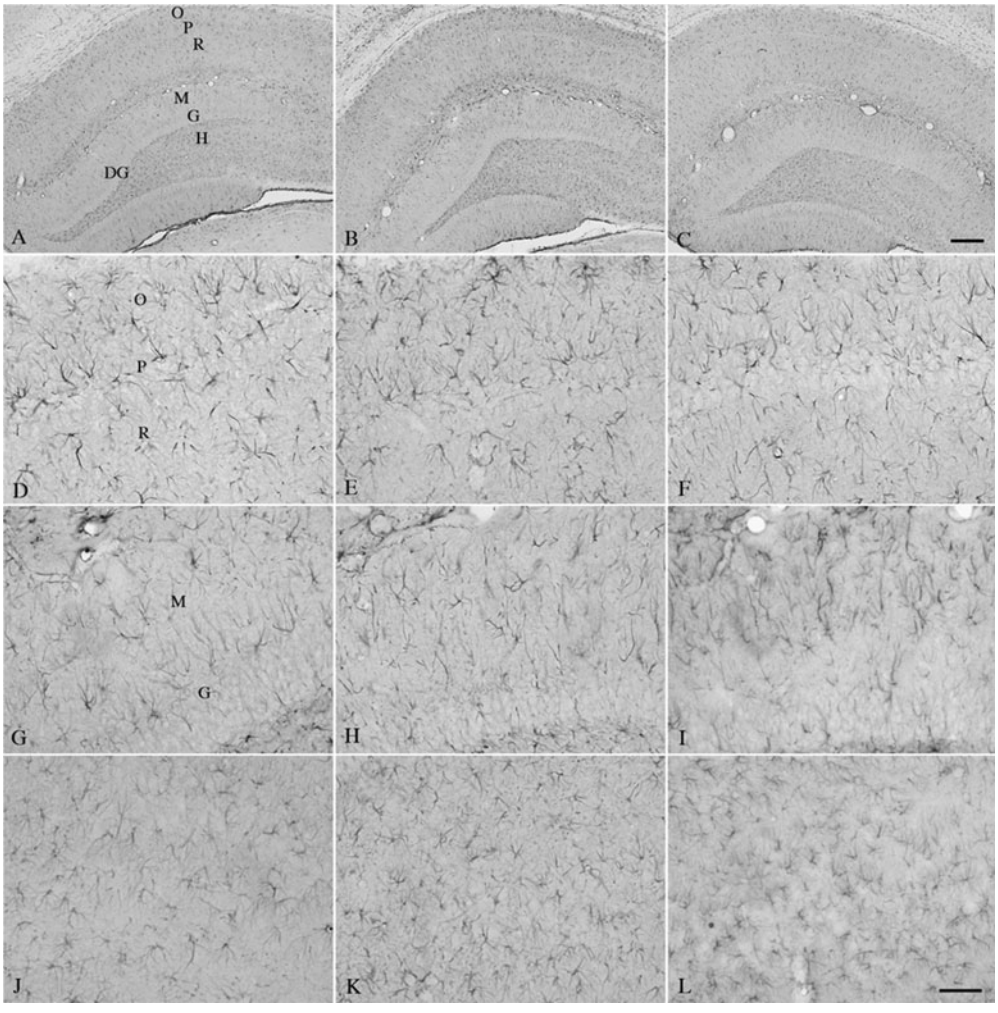

Fig. 1. Immunohistochemistry for glial fibrillary acidic protein (GFAP) in different hippocampal regions of the control group (**A**, **D**, **G**, **J**), 4 weeks after adrenalectomy (ADX) (**B**, **E**, **H**, **K**), and after 2 weeks of corticosterone replacement (2 weeks after ADX) (ADX + CORT) (**C**, **F**, **I**, **L**) under low (**A–C**) and high (**D–L**) magnification. Low-magnification photographs: GFAP-immunostaining in the hippocampus of sham-operated control group (**A**), ADX group (**B**), and following corticosterone (CORT) replacement to the ADX rat group (**C**); high-magnification photographs: stratum oriens and stratum radiatum in the sham-operated control (**D**), ADX group (**E**), and ADX with CORT replacement group (**F**); high-magnification photographs: molecular layer of dentate gyrus in the control group (**G**), the ADX group (**H**), and ADX with CORT replacement group (**I**); and high-magnification photographs: hilus of dentate gyrus in the sham-operated control (**J**), the ADX group (**K**), and ADX with CORT replacement group (**L**). Number of GFAP-immunoreactive cells and density of reactivity increased in the ADX group (**B**, **E**, **H**, **K**), in comparison with the control group (**A**, **D**, **G**, **J**). Hypertrophic astrocytes with thicker and more ramified processes were found, and some extended into the neighboring neuronal cell layer (**E**, **H**, **K**). In the ADX with CORT replacement rats (**C**, **F**, **I**, **L**), the morphology of astrocytes reverted to the control level. *DG*, dentate gyrus; *O*, stratum oriens; *P*, pyramidal cell layer; *R*, stratum radiatum; *M*, molecular cell layer; *G*, granule cell layer; *H*, hilus of dentate gyrus. *Bars* **A–C** 250 μm; **D–L** 50 μm

morphology of the astrocytes is similar in each layer, there is a slight difference from layer to layer. Astrocytes in the peripyramidal layers are small cells with many processes spread out in all directions (Fig. 1D), whereas astrocytes in the supragranular layer (molecular) of the dentate gyrus are larger than those in the other two regions, and their processes point perpendicular to the granular layer (Fig. 1G). The astrocytes in the polymorphic cell layer of the dentate gyrus are smaller with many branches pointing in all directions (Fig. 1J).

It could be readily recognized that both the number of GFAP-ir cells and the density of immunoreactivity were increased in the ADX group (Fig. 1B,E,H,K), in comparison with the sham-control group (Fig. 1A,D,G,J). The morphology of the GFAP-ir cells in all regions showed hypertrophic changes with elevated levels of GFAP. These hypertrophic findings were mainly represented by increased branching and thickness of astrocyte processes in the ADX group. The hypertrophic astrocytes neighboring the neuronal layer sent their long and thick fibrous processes into the pyramidal cell layer or granular cell layer of the dentate gyrus (Fig. 1E,H). In the corticosterone replacement group, the morphology of astrocytes recovered and appeared similar to that of the sham-control group (Fig. 1C,F,I,L).

Change in the number of GFAP-immunoreactive cells under different corticosteroid conditions

For the quantitative evaluation, the number of GFAP-ir cells was counted and statistically analyzed under different glucocorticoid conditions. GFAP-ir astrocytes with a clear distinguished nucleus and perinuclear cytoplasm or processes were counted. The number of GFAP-ir cells was calculated in three regions of the hippocampus, the peripyramidal cell layer of CA1 (stratum oriens and stratum radiatum), and the supragranular (molecular) and subgranular (polymorphic cell) layers of dentate gyrus of each group from the same section level (Fig. 2A). It was observed that the number of GFAP-ir cells was significantly increased in the ADX group, in comparison with the sham operated-control group. In summary, the number of GFAP-ir cells after ADX was significantly increased to 177%, 192%, and 187% in stratum oriens and stratum radiatum, and molecular and polymorphic cell layers of dentate gyrus, respectively, in comparison with the sham-operated control group (Fig. 2A). The total number of the three regions of GFAP-ir cells in ADX group was increased by as much as 183% of the control group (Fig. 2B). An ANOVA analysis revealed a significant difference between sham-operated control group and ADX group both in each region and in total. Corticosterone replacement to the ADX showed the reduction of the number of GFAP-ir cells to the control level in each region and the total of three regions examined (Fig. 2A,B). Statistical analysis showed that the corticosterone group did not differ significantly from the sham-operated control group.

Change in the density of GFAP-immunopositive cells under different corticosteroid conditions

The density of GFAP-ir was measured in three regions of hippocampus; the peripyramidal cell layer of CA1 (stratum oriens and stratum radiatum); and supragranular (molecular) and subgranular (polymorphic cell) layers of dentate gyrus, on each group from the same section level. Following ADX, increased GFAP reactivity was readily observed in all hippocampal subregions. The density of the GFAP-ir cells in each region measured in the ADX group was increased nearly 30% compared to the sham-operated control group (Fig. 3A). The total density of three regions

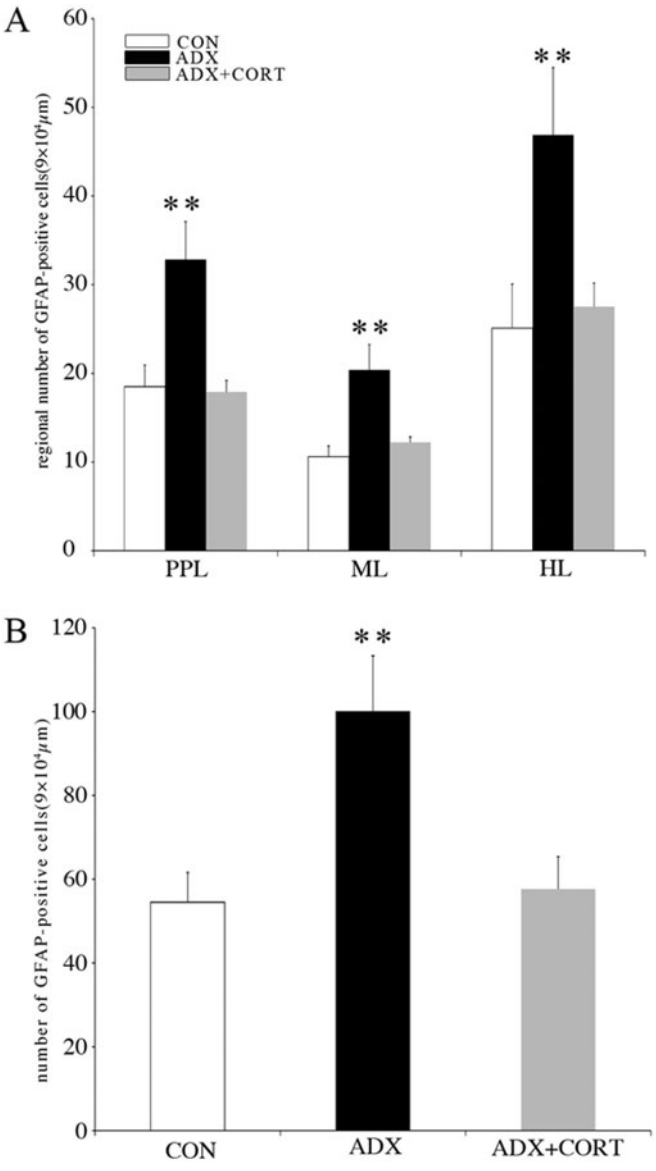

Fig. 2. **A** Number of GFAP-immunoreactive (GFAP-ir) cells in each hippocampal region. In the ADX group, the number of GFAP-ir cells was markedly increased to nearly twofold that of the sham-operated control group in peripyramidal layers (*PPL*, including stratum oriens and stratum radiatum), molecular (*ML*), and hilus of dentate gyrus (*HL*; also called polymorphic cell layers) $^{**}P < 0.01$ compared to control group. **B** Total number of GFAP-ir cells in three hippocampal regions. Total number of GFAP-ir cells in ADX group was increased in comparison with the sham-operated control group. The ADX with CORT replacement group showed a number of GFAP-ir cells similar to the control level in all regions examined. $^{**}P < 0.01$ compared to the sham-operated control group. *Error bars* represent SEM

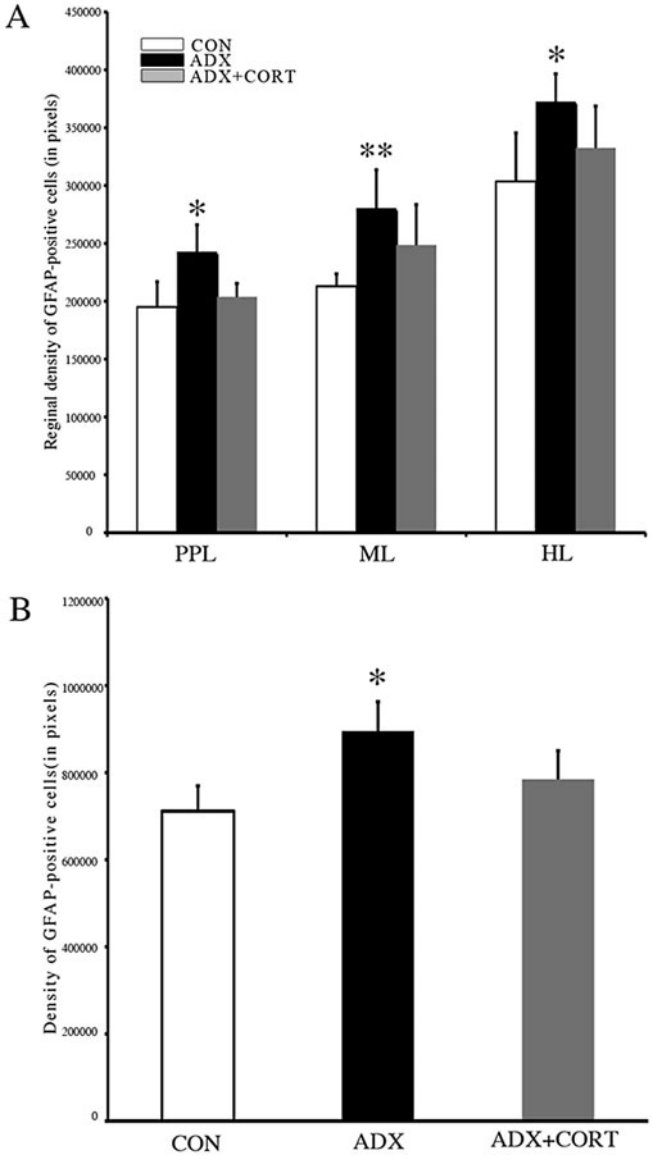

Fig. 3. **A** The density of GFAP-ir cells in each hippocampal region. After ADX, the density of GFAP-ir cells in each region increased nearly 30% compared to the controls. **B** The total density of GFAP-ir cells in three hippocampus regions. The total density of three regions was increased by nearly 30% after ADX compared to that in control. In the group of ADX with CORT replacement, the density of GFAP-ir cells returned to the state of the control level in each region. $*P < 0.05$ compared to control group. $**P < 0.01$ compared to control group. *Error bars* represent the SEM. *PPL*, peripyramidal layers; *ML*, molecular; *HL*, hilus of dentate gyrus

was also increased nearly 30% after ADX compared to the sham-operated control group (Fig. 3B). Statistical analysis revealed a significant difference between the sham-operated control group and the ADX group both in each region and in total regions. The density of GFAP-ir cells in the corticosterone replacement group was near the control level in each region and in the total of three regions (Fig. 3A,B). An ANOVA analysis showed no significant difference between the corticosterone replacement group and the sham-operated control group both in each region and in total regions.

Morphological changes of astrocytes under different corticosteroid conditions by ultra-high-voltage electron microscopy

The astrocytes prepared by Golgi impregnation were observed by ultra-high-voltage electron microscopy (UHVEM), which revealed detailed dynamic ultrastructural changes of the astrocytes (Fig. 4). The cell body markedly reacted except for the nucleus. The thick processes arose from the cell body and spread toward the periphery. Many thin irregular leaflet-like branches were observed. This complex branching often anastomosed to make a fine three-dimensional network (Fig. 4A-A′). After ADX, the size and branching of astrocytes were clearly developed. The fine mesh structure that spread out from the branching of astroglia was well developed and the three-dimensional network, formed by the anastomoses of their branching, also was well developed (Fig. 4B-B′). These hypertrophied structural changes following ADX reverted to the sham-operated control condition with corticosterone replacement (Fig. 4C-C′).

Discussion

The present study is the first to show detailed quantitative analysis for the number of GFAP-ir cells and density of GFAP immunoreactivity and the morphological changes of astrocytes in rat hippocampus under different corticosteroid conditions. The study indicated that the expression of GFAP was activated by ADX and the GFAP-ir cells showed hypertrophic changes by ADX, whereas corticosterone treatment of ADX rats facilitated return to the state of the sham-operated control condition. The morphometric changes were observed in particular around the pyramidal neurons of CA1 and in the subgranular layer of the dentate gyrus. These changes were impressively observed by UHVEM, expressing the three-dimensional ultrastructure. The astrocytes showed a more complicated fine branching three-dimensional network after ADX. These results suggested that both the structure and function of astrocytes were modulated by corticosteroids.

It is well known that corticosteroids are secreted from the adrenal cortex and bind to their receptors, therefore facilitating genomic or nongenomic effects in the brain. The hippocampus is a principal target for corticosteroids in the brain, because a higher concentration of corticosterone receptors has been observed in hippocampal neurons.[1,31] Previous studies have indicated that a chronic high level of circulating glucocorticoids induces damage to hippocampal pyramidal neurons,[32,33] whereas removal of glucocorticoids by ADX induced degeneration and death of mature granule neurons in the dentate gyrus.[15–18,33,34] These neuronal degenerations or death following ADX were suggestive of apoptosis, and the neuronal degenerative changes were reported

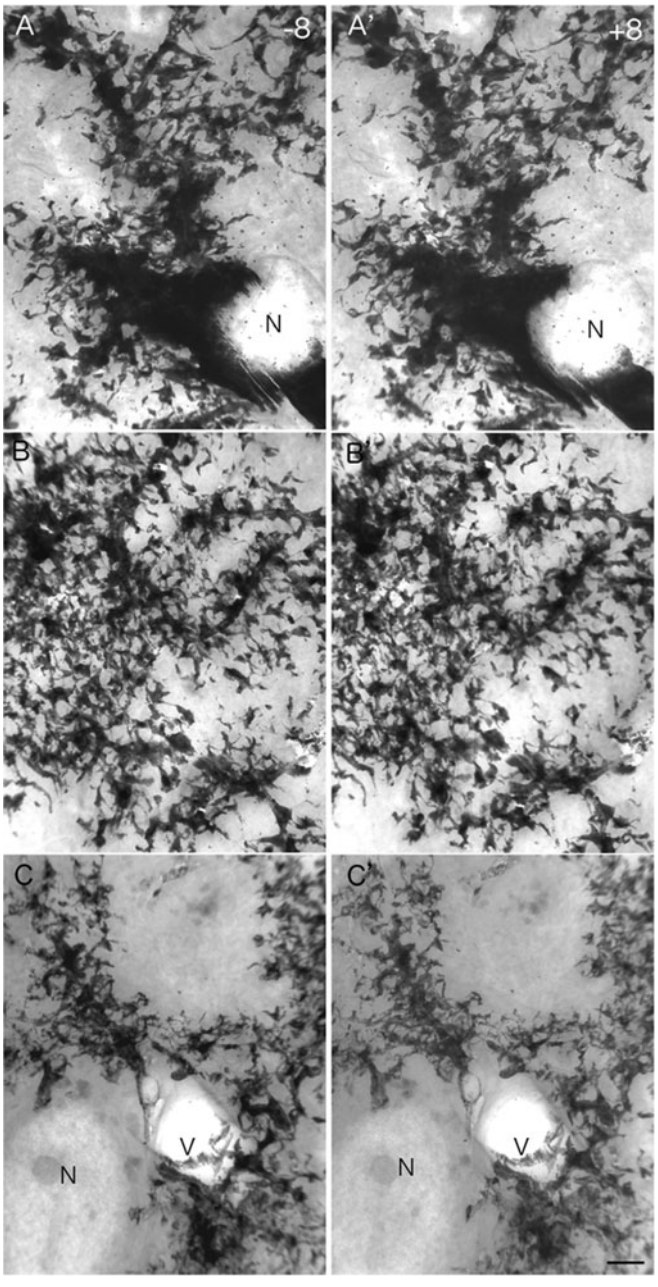

Fig. 4. Morphological changes in three groups observed by ultra-high-voltage electron microscopy (UHVEM). All the stereo-images of UHVEM showed ± 8° tilt. **A-A′** Images of sham-operated control group show that the thick processes arose from the cell body and formed complicated branching. These complex branching networks often anastomosed to make a fine three-dimensional network. **B-B′** Stereo images after ADX showed hypertrophy and well-developed fine mesh structures. **C-C′** Stereoimages of ADX rats with CORT replacement showed a morphological structure similar to that of the sham-operated control group. *N*, neuron; *V*, vessel. *Bars* 5 μm

to be prevented by corticosterone.[16,35–37] The expression of corticosteroid receptors, mineralocorticosteroid receptor (MR), and glucocorticoid receptor (GR) in astrocytes has been assessed by radioisotope-binding assay.[13] Moreover, Vielkind et al.[10] revealed that all classes of glial cells including astrocytes and oligodendrocytes expressed GR by double immunofluorescence study in vivo. In the present study we clearly demonstrated that a significant changes of GFAP-ir, a marker for astrocytes, under different corticosteroid conditions. Krugers et al.[21] indicated that adrenalectomy-induced neuronal degeneration in the rat dentate gyrus and mossy fiber zone coincides with hypertrophy of astroglia, which were consistent with our present results of hypertrophic appearance with well-developed thicker fibrous processes, strongly suggesting that the morphofunctional changes of astroglia under changing circulation of corticosteroids were closely relevant to neuronal changes.

An increase in GFAP expression in hippocampus and other region of brain following ADX was reported previously.[19–21] The present study showed a significant increase in GFAP-ir cells with ADX that is in agreement with these previous reports, but in addition some differences obtained. A previous study revealed that increase of GFAP-ir specifically confined in the dentate gyrus after ADX,[20,21] but our results confirmed the increase also in other hippocampal regions, such as the peripyramidal layer. In the present study we clearly revealed the significant increase of GFAP-ir cells both in number and density after ADX, especially in specific hippocampal areas examined: stratum oriens and stratum radiatum of the peripyramidal cell layer of CA1, and supragranular and subgranular layers of the dentate gyrus. It has been reported that glucocorticoids decrease GFAP mRNA and regulate transcription in the hippocampus and cerebral cortex.[28,38] O'Callaghan et al.[19] showed that changes in amount of GFAP caused by CORT and ADX were paralleled by changes in GFAP mRNA. Therefore, our findings of a significant increase in the number and the density of GFAP-ir cells after ADX might possibly be regulated via a genomic effect of corticosteroids.

One possible explanation for the GFAP-ir cells increase after ADX might be the astrocytic reaction to neurodegeneration induced by ADX because many previous studies reported that adrenalectomy results in neurodegeneration.[15–18] An important step of glial response to neurodegeneration is thought to be removal of cellular debris.[16] Krugers et al.[21] advocated the possibility of a neuron–glia interaction under corticosteroid regulation around the hippocampus. They demonstrated that alternation of GFAP-ir was confined to the area suffering neurodegeneration following ADX; both GFAP-ir and neurodegeneration showed a similar distribution over the hippocampus, and also showed a survival time-dependent increase after ADX, suggesting a relationship between ADX-induced neurodegeneration and the induction of GFAP-ir that alluded to the functional changes of astrocytes. Moreover, the prolonged administration of corticosterone not only attenuates the exacerbating effects of ADX but also partially reverses trimethyltin (TMT)-induced neuronal loss and reactive astrogliosis, signifying a neuroprotective action of glucocorticoid receptors in the hippocampus,[39] suggesting an association with the compensatory mechanism designed to exacerbate the neuronal condition, and supporting the hypothesis that the morphofunctional changes of astrocytes under different corticosteroid conditions are related to the neuronal changes.

In the present study, we presented the three-dimensional ultrastructural changes of astrocytes under different corticosteroid conditions as observed by UHVEM. Because glial cells as well as neurons display complicated morphological features with multiple processes, it is difficult to display all fine structures. UHVEM stereoscopy using thick sections can combine the advantages of light microscopy and conventional thin-section electron microscopy. This method has been reported to provide morphological and morphometric study of the complicated structures in the central nervous system.[30,40] Actually, the present study dynamically contributed to reveal the changes of the detailed fine structure of astrocytes, which showed thin irregular ribbon-like or leaf-like branches, arising from thick processes and anastomosing to form a complicate three-dimensional network, under different corticosteroid conditions. These observations strongly suggest the need for a careful reconsideration of the fine morphology of the astroglial terminal branches in the nervous system for understanding of the astroglia. It may be also suggested that this complicated glial branching has a more functional role than simple insulation of adjacent neurons.

In conclusion, we revealed the detailed morphofunctional changes of astrocytes in the hippocampus by employing immunohistochemistry for GFAP and morphometric analysis, and three-dimensional fine structure by UHVEM observation. These results may contribute to resolve the role of astrocytes in the neuron–glia interaction under exacerbated condition for neurons. However, the detailed complex interaction between neurons and glial cells under different corticosteroid conditions still remains to be clarified. Future studies should also concentrate on the molecular mechanism for the neuron–glia interaction under different corticosteroid conditions.

Acknowledgments This study was supported by the Naito Foundation to H.O. and the Grant-in Aid for Scientific Research from the Ministry of Education, Culture, Sports, Science and Technology (METX), Japan (to H.O., 22590230, S0801035).

References

1. McEwen BS, De Kloet ER, Rostene W (1986) Adrenal steroid receptors and actions in the nervous system. Physiol Rev 66:1121–1188
2. Aronsson M, Fuxe K, Dong Y, Agnati LF, Okret S, Gustafsson JA (1988) Localization of glucocorticoid receptor mRNA in the male rat brain by in situ hybridization. Proc Natl Acad Sci USA 85: 9331–9335
3. Reul JM, Pearce PT, Funder JW, Krozowski ZS (1989) Type I and type II corticosteroid receptor gene expression in the rat: effect of adrenalectomy and dexamethasone administration. Mol Endocrinol 3:1674–1680
4. Cintra A, Zoli M, Rosén L, Agnati LF, Okret S, Wikström A-C, Gustafsson J-Å, Fuxe K (1994) Mapping and computer assisted morphometry and microdensitometry of glucocorticoid receptor immunoreactive neurons and glial cells in the rat central nervous system. Neuroscience 62:843–897
5. De Kloet ER (1995) Steroids, stability and stress. Front Neuroendocrinol 6:416–425
6. Bas VS, Erica P, Diane H, Hans TM (1996) Partial colocalization of glucocorticoid and mineralocorticoid receptors in discrete compartments in nuclei of rat hippocampus neuron. J Cell Sci 109:787–792
7. Ito T, Morita N, Nishi M, Kawata M (2000) In vivo and in vitro immunocytochemistry for the distribution of mineralocorticoid receptor with the use of specific antibody. Neurosci Res 37:173–182
8. Han F, Ozawa H, Matsuda K, Nishi M, Kawata M (2005) Colocalization of mineralocorticoid receptor and glucocorticoid receptor in the hippocampus and hypothalamus. Neurosci Res 51:371–381
9. Fuxe K, Wikstrom A, Okret S, Agnati LF, Harfstrand A, Yu ZY, Granholm M, Zoli M, Vale W (1985) Mapping of glucocorticoid receptor immunoreactive neurons in the rat tel- and diencephalons using a monoclonal antibody against rat liver glucocorticoid receptor. Endocrinology 117:1803–1812
10. Vielkind U, Walencewicz A, Levine JM, Bohn MC (1990) Type II glucocorticoid receptors are expressed in oligodendrocytes and astrocytes. J Neurosci Res 27:360–373
11. Bohn MC, Howard E, Vielkind U, Krozowski Z (1991) Glial cells express both mineralocorticoid and glucocorticoid receptors. J Steroid Biochem Mol Biol 40:105–111
12. Chou YC, Luttge WG, Sumners C (1990) Characterization of glucocorticoid type II receptors in neuronal and glial cultures from rat brain. J Neuroendocrinol 2:29–38
13. Chou YC, Luttge WG, Sumners C (1991) Expression of mineralocorticoid type I and glucocorticoid type II receptors in astrocyte glia as a function of time in culture. Brain Res 16:55–61
14. Hwang IK, Yoo KY, Nam YS, Choi JH, Lee IS, Kwon Y-G, Kang T-C, Kim Y-S, Won MH (2006) Mineralocorticoid and glucocorticoid receptor expressions in astrocytes and microglia in the gerbil hippocampal CA1 region after ischemic insult. Neurosci Res 54:319–327
15. Sloviter RS, Valiquette G, Abrams GM, Ronk EC, Sollas AL, Paul LA, Neubort S (1989) Selective loss of hippocampal granule cells in the mature rat brain after adrenalectomy. Science 243:535–538
16. Sloviter RS, Sollas AL, Dean E, Neubort S (1993) Adrenalectomy-induced granule cell degeneration in the rat hippocampal dentate gyrus: characterization of an in vivo model of controlled neuronal death. J Comp Neurol 330:324–336
17. Nichols NR, Masters JN, Finch CE (1994) Cloning of steroid responsive mRNAs by differential hybridization. Methods Neurosci 22:296–313
18. Masters JN, Cotman SL, Osterberg HH, Nichols NR, Finch CE (1996) Modulation of a novel RNA in brain neurons by glucocorticoid and mineralocorticoid receptors. Neuroendocrinology 63:28–38
19. O'Callaghan JP, Brinton RE, McEwen BS (1991) Glucocorticoids regulate the synthesis of glial fibrillary acidic protein in intact and adrenalectomized rats but do not affect its expression following brain injury. J Neurochem 57:860–869
20. Gould E, Cameron HA, Daniels DC, Woolley CS, McEwen BS (1992) Adrenal hormones suppress cell division in the adult rat dentate gyrus. J Neurosci 12:3642–3650
21. Krugers HJ, Medema RM, Postema F, Korf J (1994) Induction of glial fibrillary acidic protein immunoreactivity in the rat dentate gyrus after adrenalectomy: comparison with neurodegenerative changes using silver impregnation. Hippocampus 4:307–314
22. Smith SJ (1994) Neural signaling. Neuromodulatory astrocytes. Curr Biol 4:807–810
23. Araque A, Parpura V, Sanzgiri RP, Haydon PG (1999) Tripartite synapses: glia, the unacknowledged partner. Trends Neurosci 22:208–215
24. LoTurco JJ (2000) Neural circuits in the 21st century: synaptic networks of neurons and glia. Proc Natl Acad Sci USA 97:8196–8197
25. Parpura V, Haydon PG (2000) Physiological astrocytic calcium levels stimulate glutamate release to modulate adjacent neurons. Proc Natl Acad Sci USA 97:8629–8634
26. Haydon PG (2001) Glia: Listening and talking to the synapse. Nat Rev Neurosci 2:185–193
27. Fieles RD, Stevens B (2002) New insights into neuron–glia communication. Science 298:556–562
28. Nichols NR, Osterburg HH, Masters JN, Millar SL, Finch CE (1990) Messenger RNA for glial fibrillary acidic protein is decreased in rat brain following acute and chronic corticosterone treatment. Mol Brain Res 7:1–7

29. Nichols NR, Agolley D, Zieba M, Bye N (2005) Glucocorticoid regulation of glial responses during hippocampal neurodegeneration and regeneration. Brain Res Rev 48:287–301
30. Hama K, Arii T, Kosaka T (1994) Three-dimensional organization of neuronal and glial processes: high voltage electron microscopy. Microsc Res Tech 29:357–367
31. Morimoto M, Morita N, Ozawa H, Yokoyama K, Kawata M (1996) Distribution of glucocorticoid receptor immunoreactivity and mRNA in the rat brain: an immunohistochemical and in situ hybridization study. Neurosci Res 26:235–269
32. Sapolsky RM, Krey LC, McEwen BS (1985) Prolonged glucocorticoid exposure reduces hippocampal neuron number: implication for aging. J Neurosci 5:1222–1227
33. Gould E, Woolley CS, McEwen BS (1990) Short-term glucocorticoid manipulations affect neuronal morphology and survival in the adult dentate gyrus. Neuroscience 37:367–375
34. Hu ZT, Yuri K, Ozawa H, Lu HP, Kawate M (1997) The in vivo time course for elimination of adrenalectomy-induced apoptosis profiles from the granule cell layer of the rat hippocampus. J Neurosci 17:3981–3989
35. Kerr JFR, Wyllie AH, Currie AK (1972) Apoptosis: a basic biological phenomenon with wide-ranging implications in tissue kinetics. Br J Cancer 28:239–257
36. Wyllie AH (1980) Glucocorticoid-induced thymocyte apoptosis is associated with endogenous endonuclease activation. Nature (Lond) 284:555–556
37. Arends MD, Morris RG, Wyllie AH (1990) Apoptosis: the role of the endonuclease. Am J Pathol 136:593–608
38. Laping NJ, Nichols NR, Day JR, Johnson SA, Finch CE (1994) Transcriptional control of glial fibrillary acidic protein and glutamine synthetase in vitro shows opposite responses to corticosterone in the hippocampus. Endocrinology 135:1928–1933
39. Imai H, Nishimura T, Sadamatsu M, Liu Y, Kabuto M, Kato N (2001) Type II glucocorticoid receptors are involved in neuronal death and astrocyte activation induced by trimethyltin in the rat hippocampus. Exp Neurol 171:22–28
40. Hama K, Arii T, Kosaka T (1989) Three-dimensional morphometrical study of dendritic spines of the granule cell in the rat dentate gyrus with HVEM stereo image. J Electron Microsc Tech 12: 80–87